Efficient Iterative Estimation of the Parameters of a Damped Complex Exponential in Noise

Elias Aboutanios, *Senior Member, IEEE* and Shanglin Ye, *Student Member, IEEE*

***Abstract*—The estimation of the frequency and decay factor of a single decaying exponential in noise is a problem of prime importance. A popular estimation scheme uses the computationally efficient implementation of the Fourier transform, the FFT, to obtain a coarse estimate which is then improved by a fine estimation stage. Such estimators, however, show a performance that degrades and departs from the Cramer Rao Lower Bound (CRLB) as the number of samples increases. In this paper, we propose an iterative, exponentially windowed algorithm that overcomes this problem. We derive the new estimator's theoretical performance and study its behaviour under different decay rates of the window. We show that the estimator has excellent performance that tracks the CRLB with increasing sample number and signal to noise ratio if the window decay rate is appropriately set.**

***Index Terms*—NMR spectroscopy, parameter estimation, DFT interpolation, damped exponential.**

I. Introduction

DECAYING exponentials appear in many physical processes and the estimation of their parameters is an important research topic, [1], [2], [3]. In this work we focus on the estimation of the frequency and decay factor of a single damped exponential in additive white noise. We are interested in robust, efficient, yet computationally simple estimators. The signal model we are concerned with is

$$x[k] = s[k] + w[k],\ k = 0 \dots N-1, \tag{1}$$

where the signal of interest $s[n]$ is an exponential of the form

$$s[k] = Ae^{(-\eta + j2\pi f)k} = Az^k. \tag{2}$$

Here η is the decay factor, and the frequency f is normalised by the sampling frequency, i.e. $f \in [-0.5, 0.5]$. The complex amplitude $A = |A|e^{j\phi}$, ϕ being the initial phase, is treated as a nuisance parameter. The noise terms, $w[k]$, are zero mean, complex additive white Gaussian with variance σ^2, giving a nominal signal to noise ratio (SNR) $\rho_0 = \frac{|A|^2}{\sigma^2}$, [1]. Our aim is to obtain estimates of f and η from a block of N samples. The Cramer Rao Lower Bounds (CRLBs) for the frequency, σ_f^2, and decay factor, σ_η^2, are given by, [4]

$$\begin{aligned}\sigma_\eta^2 &= 4\pi^2\sigma_f^2 \\ &= \frac{(1-|z|^2)^3(1-|z|^{2N})}{2\rho_0\left[-N^2|z|^{2N}(1-|z|^2)^2 + |z|^2(1-|z|^{2N})^2\right]}.\end{aligned} \tag{3}$$

The authors are with the School of Electrical Engineering and Telecommunications, The University of New South Wales, Building G17, Sydney, NSW, Australia, 2052, phone: +61 2 9385 5010, fax: +61 2 9385 5993 , e-mail: elias@ieee.org.

Part of this work has been accepted in EUSIPCO 2013.

Many approaches exist for obtaining these estimates and a recent review of these techniques is presented in [3]. Sums of multiple exponentials are usually treated using high resolution techniques, [5], [6], [7], [8]. Although these methods can be reasonably accurate, especially when the number of sinusoids is known, they are computationally expensive and inefficient when applied to a single exponential. This makes them at the very least unattractive, and at worst impractical when the number of samples and/or components is large. It is therefore no surprise that Discrete Fourier Transform (DFT) based estimators are best suited to this problem in the case of a large number of samples due to their robustness and computational efficiency, [3].

The maximiser of the DFT has been shown to give the maximum likelihood estimate of the frequency of an undamped complex exponential in additive Gaussian noise, [9], [10]. The maximisation of the DFT, however, is a computationally intensive step that is usually approximated by the sampled DFT that is calculated using the highly computationally efficient fast Fourier transform (FFT), [9]. Since the FFT-based estimate is coarse (of order N) with respect to the CRLB (which is of order $N^{-3/2}$), an interpolation step is necessary in order to refine the resulting estimate, [10], [11]. Although no efficient estimator exists for the damped case, [12], this approach has also proven itself to be effective for the estimation of the frequency and decay factor of a damped exponential, [1], [13], [14]. A distinguishing aspect of the method proposed in [1], which we refer to as the A&M estimator, is that it can be implemented iteratively, which permits it to achieve the minimum variance for the methods belonging to its class.

One fundamental problem afflicting these methods in the damped case is that their performance can significantly depart from the CRLB as N increases. Whereas the CRLB flattens out as a function of N, the performance of the practical estimators can even exhibit an increase in variance due to the degradation of the effective signal to noise ratio, [1], [3]. In fact, it was found in [1] that an optimum number of samples exists that gives the best estimation variance. In this paper we study a new windowing strategy that allows the performance of the algorithms to track the CRLB as it does in the undamped case, [15]. We derive its theoretical performance and assert the fact that the decay factor of the exponential window should be properly chosen in order to obtain the optimal performance.

The rest of the paper is organised as follows: In Section II we present the windowed estimation algorithm and discuss its implementation. In Section III we analyse and evaluate the theoretical performance of the estimator. In Section IV we propose a practical strategy for iteratively implementing the

estimator. Simulation results in section V show the effectiveness of the new technique. Finally, some conclusions are drawn in section VI.

II. Exponentially Windowed Estimator

The DFT represents a signal as a weighted sum of undamped sinusoids and is therefore not well suited for damped signals, [7]. As the decay factor increases, the main lobe is increasingly broadened. Thus, the authors of [16] suggest improving the representation of the DFT in the case of a damped exponential by pre-multiplying the signal with Gaussian window of the form $\nu_G[k] = e^{\gamma_0 k - \gamma_1 k^2}$, such that $\gamma_0, \gamma_1 \geq 0$. They also note that the best resolution is obtained when γ_0 is equal to the decay factor of the component of interest, but give no indication as to the choice of γ_1. In fact, they point out that since the decay factor is unknown a-priori, manual tuning of the parameters γ_0 and γ_1 is required to obtain the best resolution.

Whereas multiplying the signal with an exponentially rising window improves the sharpness of the DFT representation of a noiseless damped exponential (as it removes the decay), it also amplifies the noise at the tail end of the signal resulting in significant degradation in the effective SNR. Even without the application of a rising window, the effective SNR has been shown in [1] to decrease as the number of samples increases beyond a certain value. This behaviour is reflected in the estimation performance of the interpolation algorithms as they initially track the CRLB but then depart from it as N gets larger, [1]. This is the result of the signal nearly vanishing for large N leaving only noise. This led us to consider in [15] applying a decaying window to the signal that reduces the contribution of those samples with low SNR. A natural choice is an exponential window of the form $\nu[k] = e^{-\gamma k}$, such that $\gamma \geq 0$. Our goal is to establish whether this approach improves the performance and to determine the optimal value for the window decay factor γ is.

Throughout the paper we denote by $\hat{\bullet}$ the estimate of the parameter $\bullet$. We start by the derivation of the estimators assuming the exponential window. The DFT coefficients of the damped sinusoid are

$$\begin{aligned} X[n] &= \frac{1}{N}\sum_{k=0}^{N-1} s[k]\nu[k]e^{-j2\pi\frac{kn}{N}} \\ &= \frac{1}{N}\sum_{k=0}^{N-1} Ae^{(-\eta+j2\pi f)k}e^{-\gamma k}e^{-j2\pi\frac{kn}{N}} \\ &= \frac{1}{N}\sum_{k=0}^{N-1} Ae^{(-(\eta+\gamma)+j2\pi f)k}e^{-j2\pi\frac{kn}{N}} \\ &= \frac{1}{N}\sum_{k=0}^{N-1} s_\gamma[k]e^{-j2\pi\frac{kn}{N}}. \end{aligned}$$

Thus the DFT of the windowed signal can be viewed as the DFT of a new damped exponential $s_\gamma[k]$ with a decay factor $\eta+\gamma$. Thus, provided that the estimators of [1] remain statistically well-behaved, they can be used to obtain the parameters of $s_\gamma[k]$. We briefly review the A&M estimator here and then proceed in the next section to establish its statistical properties.

Let $\alpha = N(\eta+\gamma)$ and $f = \frac{m+\delta}{N}$, where m is the periodogram maximum and $\delta \in [-0.5, 0.5]$. For high enough SNR (see [1]), the coarse estimation stage of the algorithm returns m. Putting $z_\gamma = e^{\frac{-\alpha+j2\pi\delta}{N}}$, we can obtain $\hat{z}_\gamma$ from

$$\hat{z}_\gamma = \frac{1}{\cos\left(\frac{\pi}{N}\right) - 2jh\sin\left(\frac{\pi}{N}\right)}, \tag{4}$$

where the interpolation function is given by

$$h = \frac{1}{2}\frac{X_{0.5} + X_{-0.5}}{X_{0.5} - X_{-0.5}}, \tag{5}$$

and $X_p \equiv X[m+p]$. Since it is simpler to obtain $\hat{z}_\gamma^{-1} = e^{\frac{\alpha-j2\pi\delta}{N}}$, the estimates $\hat{\eta}$ and $\hat{\delta}$ expressed in terms of $\hat{z}_\gamma^{-1}$ become, [1],

$$\hat{\eta} = \frac{\hat{\alpha}}{N} - \gamma = -\ln\left(\hat{z}_\gamma\right) - \gamma, \quad \text{and} \quad \hat{\delta} = -\frac{N}{2\pi}\angle\hat{z}_\gamma. \tag{6}$$

It is worth noting that the above expressions contain highly non-linear functions which may be undesirable in certain implementations. A number of computational simplifications, leading to different biases, are possible (see [1]).

III. Theoretical Analysis

In this section, we present theoretical analysis of the windowed estimator. The DFT coefficient X_p ($p = \pm 0.5$), with the noise terms included, can be expressed as

$$\begin{aligned} X_p &= c_\gamma \frac{1}{N\left(1 - e^{\frac{-\alpha+j2\pi(\delta-p)}{N}}\right)} + W_p \\ &= c_\gamma \frac{1}{N\left(1 - z_\gamma e^{-j\frac{2\pi p}{N}}\right)} + W_p \end{aligned} \tag{7}$$

where

$$c_\gamma = A\left(1 + e^{-\alpha+j2\pi\delta}\right). \tag{8}$$

The terms W_p are the DFT coefficients of the noise

$$\begin{aligned} W_p &= \frac{1}{N}\sum_{k=0}^{N-1} w[k]\nu[k]e^{-j2\pi\frac{kn}{N}} \\ &= \frac{1}{N}\sum_{k=0}^{N-1} w[k]e^{(-\gamma-j2\pi\frac{n}{N})k}. \end{aligned}$$

No asymptotic theory can be obtained in the damped case, so we proceed to examine the small sample performance and derive an approximate expression for the estimation variance under the assumption of a sufficiently high effective SNR, [1].

A. Statistical Properties of the Noise Coefficients

Let us first examine the effect of the window on the variances of the noise coefficients. As these are no longer uncorrelated, we derive their mean, variance and covariance. Starting with the mean, we have that

$$\begin{aligned} \mathrm{E}\left[W_p\right] &= \frac{1}{N}\mathrm{E}\left[\sum_{k=0}^{N-1} w[k]e^{(-\gamma-j2\pi\frac{m+p}{N})k}\right] \\ &= \frac{1}{N}\sum_{k=0}^{N-1} \mathrm{E}\left[w[k]\right]e^{(-\gamma-j2\pi\frac{m+p}{N})k} \\ &= 0. \end{aligned} \tag{9}$$

The variance, on the other hand, is given by

$$\begin{aligned}\sigma_w^2 &= \mathrm{E}\left[|W_p|^2\right] \\ &= \mathrm{E}\left[\frac{1}{N}\left(\sum_{k=0}^{N-1} w[k]e^{\left(-\gamma-j2\pi\frac{m+p}{N}\right)k}\right)\right. \\ &\qquad \left.\frac{1}{N}\left(\sum_{l=0}^{N-1} w[l]e^{\left(-\gamma-j2\pi\frac{m+p}{N}\right)l}\right)^*\right] \\ &= \frac{1}{N^2}\sum_{k=0}^{N-1}\sum_{l=0}^{N-1}\mathrm{E}\left[w[k]w^*[l]\right]e^{-(k+l)\gamma-j2\pi\frac{m+p}{N}(k-l)} \\ &= \frac{1}{N^2}\sum_{k=0}^{N-1}\sum_{l=0}^{N-1}\sigma^2\delta_{kl}e^{-(k+l)\gamma-j2\pi\left(\frac{m+p}{N}\right)(k-l)} \\ &= \frac{\sigma^2}{N^2}\sum_{k=0}^{N-1}e^{-2k\gamma} \\ &= \frac{\sigma^2}{N^2}\frac{1-e^{-2N\gamma}}{1-e^{-2\gamma}}. \end{aligned} \tag{10}$$

Proceeding with similar mathematical argument, the covariance of the coefficients W_p and W_{p-1} is

$$\begin{aligned}\chi_w &= \mathrm{E}\left[W_p W_{p-1}^*\right] = \left(\mathrm{E}\left[W_p^* W_{p-1}\right]\right)^* \\ &= \mathrm{E}\left[\frac{1}{N}\left(\sum_{k=0}^{N-1} w[k]e^{\left(-\gamma-j2\pi\frac{m+p}{N}\right)k}\right)\right. \\ &\qquad \left.\frac{1}{N}\left(\sum_{l=0}^{N-1} w[l]e^{\left(-\gamma-j2\pi\frac{m+p-1}{N}\right)l}\right)^*\right] \\ &= \frac{\sigma^2}{N^2}\sum_{k=0}^{N-1}e^{\left(-2\gamma-j\frac{2\pi}{N}\right)k} \\ &= \frac{\sigma^2}{N^2}\frac{1-e^{-2N\gamma}}{1-e^{-2\gamma-j\frac{2\pi}{N}}}. \end{aligned} \tag{11}$$

Now that we have the statistical moments of the noise, we can obtain the estimation variance of the windowed estimator.

B. Theoretical Variance

For notational simplicity, we put $X_\pm = X_{\pm 0.5}$. The interpolation function, with the noise terms included, becomes

$$\begin{aligned}\tilde{h} &= \frac{1}{2}\frac{X_+ + X_-}{X_+ - X_-} \\ &= \frac{1}{2}\frac{\frac{c_\gamma}{N\left(1-z_\gamma e^{-j\frac{\pi}{N}}\right)} + W_+ + \frac{c_\gamma}{N\left(1-z_\gamma e^{j\frac{\pi}{N}}\right)} + W_-}{\frac{c_\gamma}{N\left(1-z_\gamma e^{-j\frac{\pi}{N}}\right)} + W_+ - \frac{c_\gamma}{N\left(1-z_\gamma e^{j\frac{\pi}{N}}\right)} - W_-} \\ &= \frac{1 - z_\gamma\cos\left(\frac{\pi}{N}\right) + \frac{N\lambda_\gamma}{2c}\left(W_+ + W_-\right)}{-j2z_\gamma\sin\left(\frac{\pi}{N}\right)\left[1 + j\frac{N\lambda_\gamma}{2cz_\gamma\sin\left(\frac{\pi}{N}\right)}\left(W_+ - W_-\right)\right]}, \end{aligned} \tag{12}$$

where

$$\lambda_\gamma = \left(1 - z_\gamma e^{-j\frac{\pi}{N}}\right)\left(1 - z_\gamma e^{j\frac{\pi}{N}}\right). \tag{13}$$

Now recall from Eq. (4) that we can express h in terms of z_γ as

$$h = \frac{1 - z_\gamma\cos\left(\frac{\pi}{N}\right)}{-2jz_\gamma\sin\left(\frac{\pi}{N}\right)}. \tag{14}$$

Therefore, the expression for $\tilde{h}$ becomes

$$\tilde{h} = \frac{h + j\frac{N\lambda_\gamma}{4c_\gamma z_\gamma\sin\left(\frac{\pi}{N}\right)}\left(W_+ + W_-\right)}{1 + j\frac{N\lambda_\gamma}{2c_\gamma z_\gamma\sin\left(\frac{\pi}{N}\right)}\left(W_+ - W_-\right)}. \tag{15}$$

Under the assumption of sufficiently high SNR, see [1], we have that $\left|W_p/A\right| \ll 1$. Thus

$$\begin{aligned}\tilde{h} &\approx \left[h + j\frac{N\lambda_\gamma}{4c_\gamma z_\gamma\sin\left(\frac{\pi}{N}\right)}\left(W_+ + W_-\right)\right] \\ &\quad \times\left[1 - j\frac{N\lambda_\gamma}{2c_\gamma z_\gamma\sin\left(\frac{\pi}{N}\right)}\left(W_+ - W_-\right)\right]. \end{aligned}$$

Expanding the above expression and ignoring the lower order terms (that is the terms of order $\left|W_p/A\right|^2$), we arrive after the necessary manipulations at

$$\tilde{h} \approx h + j\frac{N\lambda_\gamma}{4c_\gamma z_\gamma\sin\left(\frac{\pi}{N}\right)}\left[(1-2h)\,W_+ + (1+2h)\,W_-\right]. \tag{16}$$

The error in the estimation of h that is due to the noise, $\epsilon = \tilde{h} - h$ is then given by

$$\begin{aligned}\epsilon &\approx j\frac{N\lambda_\gamma}{4c_\gamma z_\gamma\sin\left(\frac{\pi}{N}\right)}\left[(1-2h)\,W_+ + (1+2h)\,W_-\right] \\ &= j\frac{N\lambda_\gamma}{4c_\gamma z_\gamma\sin\left(\frac{\pi}{N}\right)}U, \end{aligned} \tag{17}$$

where $U = (1-2h)W_+ + (1+2h)W_-$. The quantities λ_γ and c_γ are given by Eq. (13) and Eq. (8) respectively. In order to arrive at the errors in η and δ, namely μ and θ respectively, it is simpler to carry out the analysis using $\hat{z}_\gamma^{-1}$. Let the error in $\hat{z}_\gamma^{-1}$ be denoted by ζ. Then we have that

$$\zeta = -2j\epsilon\sin\left(\frac{\pi}{N}\right). \tag{18}$$

Now if we expand $\ln\left(\hat{z}_\gamma^{-1}\right)$ as Taylor series around $\ln\left(z_\gamma^{-1}\right)$ we have

$$\begin{aligned}\ln\left(\hat{z}_\gamma^{-1}\right) &= \hat{\eta} + \gamma - j\frac{2\pi}{N}\hat{\delta} \\ &= \ln\left(z_\gamma^{-1}\right) + z_\gamma\zeta + O\left[(z_\gamma\zeta)^2\right] \\ &\approx \eta + \gamma - j\frac{2\pi}{N}\delta + z_\gamma\zeta. \end{aligned} \tag{19}$$

This leads to

$$\begin{aligned}\mu - j\frac{2\pi}{N}\theta &\approx z_\gamma\zeta \\ &= -2jz_\gamma\epsilon\sin\left(\frac{\pi}{N}\right) \\ &\approx \frac{N\lambda_\gamma}{2c_\gamma}U. \end{aligned} \tag{20}$$

Equating the real and imaginary parts yields

$$\mu \approx \frac{N}{2}\mathcal{R}\left(\frac{\lambda_\gamma}{c_\gamma}U\right) \quad \text{and} \quad \theta \approx -\frac{N^2}{4\pi}\mathcal{I}\left(\frac{\lambda_\gamma}{c_\gamma}U\right). \tag{21}$$

Now it is clear that μ and θ are zero-mean. Their variances are calculated as follows; consider μ first

$$\begin{aligned}\mu &\approx \frac{N}{2}\mathcal{R}\left(\frac{\lambda_\gamma}{c_\gamma}U\right)\\ &= \frac{N}{2|c_\gamma|^2}\mathcal{R}\left(c_\gamma^*\lambda_\gamma U\right)\\ &= \frac{N}{4|c_\gamma|^2}\left(c_\gamma^*\lambda_\gamma U + c_\gamma\lambda_\gamma^* U^*\right). \end{aligned} \quad (22)$$

Then the variance of μ becomes

$$\mathrm{Var}_\gamma[\mu] \approx \frac{N^2}{16|c_\gamma|^4}\mathrm{E}\left[\left|c_\gamma^*\lambda_\gamma U + c_\gamma\lambda_\gamma^* U^*\right|^2\right]. \quad (23)$$

Carrying out the required manipulations, and noting that $\mathrm{E}\left[U^2\right] = \mathrm{E}\left[(U^*)^2\right] = 0$, we arrive at

$$\mathrm{Var}_\gamma[\mu] \approx \frac{N^2|\lambda_\gamma|^2}{8|c_\gamma|^2}\mathrm{E}\left[|U|^2\right].$$

Looking at the various terms in the above expression we have

$$\begin{aligned}\mathrm{E}\left[|U|^2\right] &= |1-2h|^2\,\mathrm{E}\left[|W_+|^2\right] + |1+2h|^2\,\mathrm{E}\left[|W_-|^2\right]\\ &\quad + (1-2h)(1+2h)^*\mathrm{E}\left[W_+W_-^*\right]\\ &\quad + (1-2h)^*(1+2h)\mathrm{E}\left[W_+^*W_-\right]\\ &= \left(|1-2h|^2 + |1+2h|^2\right)\sigma_w^2\\ &\quad + 2\mathcal{R}\left\{(1-2h)(1+2h)^*\chi_w\right\}, \end{aligned} \quad (24)$$

where σ_w^2 and χ_w are given in Eqs. (10) and (11). Furthermore, we have that

$$\begin{aligned}|1-2h|^2 &= \frac{\left|1 - z_\gamma e^{-j\frac{\pi}{N}}\right|^2}{|z_\gamma|^2\sin^2\left(\frac{\pi}{N}\right)},\\ |1+2h|^2 &= \frac{\left|1 - z_\gamma e^{j\frac{\pi}{N}}\right|^2}{|z_\gamma|^2\sin^2\left(\frac{\pi}{N}\right)}, \text{ and}\\ (1-2h)(1+2h)^* &= -\frac{\left(1 - z_\gamma e^{-j\frac{\pi}{N}}\right)\left(1 - z_\gamma^* e^{-j\frac{\pi}{N}}\right)}{|z_\gamma|^2\sin^2\left(\frac{\pi}{N}\right)}. \end{aligned}$$

Substituting these expressions into that of $\mathrm{E}\left[|U|^2\right]$ and simplifying yields

$$\mathrm{E}\left[|U|^2\right] = 2\frac{\sigma^2}{N^2}\frac{\left(1 - e^{-2N\gamma}\right)}{|z_\gamma|^2\sin^2\left(\frac{\pi}{N}\right)}\beta, \quad (25)$$

where β is shown in Eq. (26). Using the expressions for c_γ and λ_γ leads to the variance being

$$\begin{aligned}\mathrm{Var}_\gamma[\mu] &\approx \frac{\sigma^2}{4|A|^2}\frac{\left(1 - e^{-2N\gamma}\right)}{|z_\gamma|^2\sin^2\left(\frac{\pi}{N}\right)}\frac{\left|1 - 2z_\gamma\cos\left(\frac{\pi}{N}\right) + z_\gamma^2\right|^2}{|1+z_\gamma^N|^2}\beta\\ &= \frac{\left(1 - e^{-2N\gamma}\right)}{4\rho_0|z_\gamma|^2\sin^2\left(\frac{\pi}{N}\right)}\left|\frac{1 - 2z_\gamma\cos\left(\frac{\pi}{N}\right) + z_\gamma^2}{1+z_\gamma^N}\right|^2\beta \end{aligned} \quad (27)$$

The variance of θ is easily obtained from that of μ using the fact that $\mathrm{Var}_\gamma[\theta] = \frac{N^2}{4\pi^2}\mathrm{Var}_\gamma[\mu]$. Finally, the variances of $\hat{f}$ and $\hat{\eta}$ are given by:

$$\mathrm{Var}_\gamma[\hat{f}] = \frac{1}{N^2}\mathrm{Var}_\gamma[\theta]; \quad \mathrm{Var}_\gamma[\hat{\eta}] = \mathrm{Var}_\gamma[\mu]. \quad (28)$$

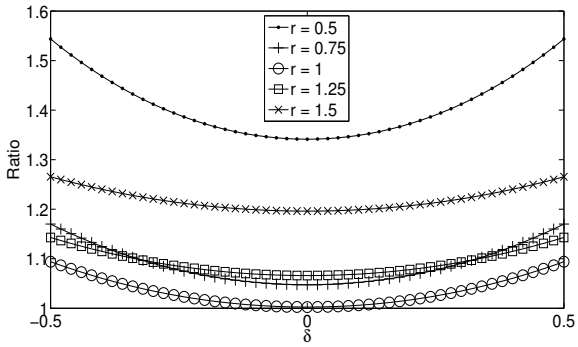

Fig. 1. Plot of the ratios of the theoretical variance of η to the CRLB versus δ under different values of r ($\eta = 0.02, N = 512, \rho_0 = 40$dB).

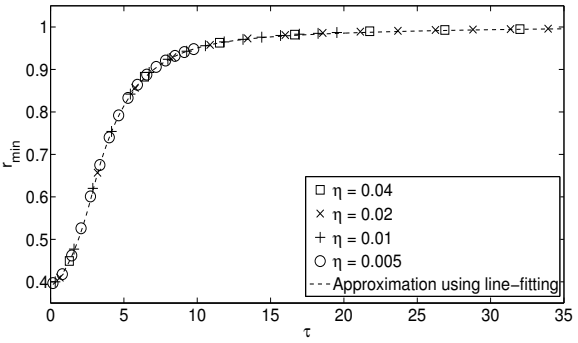

Fig. 2. Plot of $r_{\min}$ versus τ and the line-fitting curve ($\rho_0 = 40$dB).

C. Performance Discussion

Now we turn to the discussion of the estimation performance. To this end we put $r = \gamma/\eta$. We first examine the variance as a function of δ. Fig. 1 shows the ratio of $\mathrm{Var}_\gamma[\hat{\eta}]$ to the CRLB under different values of r for $\eta = 0.02$, $N = 512$ and $\rho_0 = 40$dB. We see that, although different values of r lead to different performance curves, these curves still share the same characteristic as the A&M estimator, with the ratio always exhibiting a maximum at $\delta = \pm 0.5$ and a minimum at $\delta = 0$.

Next we examine the optimal value of r that gives the best estimation performance. The fact that the estimation performance depends on the effective SNR suggests that it is a function of the product $\tau = N\eta$, rather than η or N individually. This is confirmed in Figs. 2 and 3. Fig. 2 shows the value of r, $r_{\min}$, that gives the minimum estimation variance versus τ whereas Fig. 3 gives the ratio of the estimation variance to the CRLB. The nominal SNR ρ_0 was set to 40dB, and curves for four different values of η are given. It is clear that regardless of the value of η, the same curve is always observed in both graphs. Therefore, we write $r_{\min} = f(\tau)$ and seek to determine the function $f(\tau)$. Analytically this is obtained by differentiating the variance expressions in (28) and setting the result equal to 0. However, this is a tedious and unnecessary exercise on very complicated expressions. Alternatively, we derive the function through line fitting.

Before proceeding with a determination of $f(\tau)$, we give some more insight into the behaviour of the estimator. Fig. 2

$$\beta = \frac{1 - 2\mathcal{R}\left(z_\gamma\right)\cos\left(\frac{\pi}{N}\right) + |z_\gamma|^2}{1 - e^{-2\gamma}} - \frac{1 - |z_\gamma|^2 e^{-2\gamma} - 2\left(1 - e^{-2\gamma}\right)\mathcal{R}\left(z_\gamma\right)\cos\left(\frac{\pi}{N}\right) + \left(|z_\gamma|^2 - e^{-2\gamma}\right)\cos\left(\frac{2\pi}{N}\right)}{1 + e^{-4\gamma} - 2e^{-2\gamma}\cos\left(\frac{2\pi}{N}\right)} \tag{26}$$

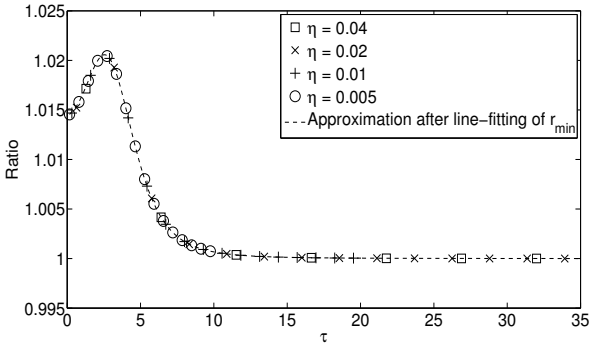

Fig. 3. Plot of the ratios of the minimum variance of η to the CRLB versus τ and the approximation curve after line-fitting of $r_{\min}$ (ρ_0 = 40dB).

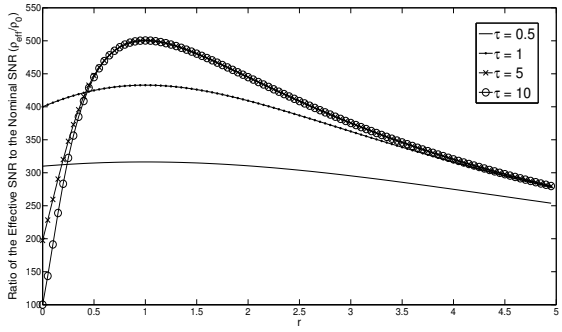

Fig. 4. Plot of the ratios of effective SNR and nominal SNR as a function of r under different values of τ (η = 0.001).

shows that $r_{\min}$ is a monotonically increasing function of τ that tends towards 1 for large τ. It is interesting to observe that as τ decreases, which in this case means a decrease in the number of samples, $r_{\min}$ decreases towards 0.4 instead of remaining at 1. This behaviour results from the interplay between the effective SNR and the cross-correlation of the DFT coefficients of the noise. Recall that the cross-correlation was derived in Eq. (11). The effective SNR, on the other hand, is given by the ratio of the true maximum of the periodogram to the noise power, [1]. It is obtained by setting $p = \delta$ in (7) and combining it with (10),

$$\rho_{\text{eff}}(r) = \frac{|X_\delta|^2}{\sigma_w^2} = \rho_0 \frac{\left(1 - e^{-(1+r)\tau}\right)^2}{1 - e^{-2r\tau}} \cdot \frac{1 - e^{-2r\eta}}{\left(1 - e^{-(1+r)\eta}\right)^2}. \tag{29}$$

The plots of the effective SNR and magnitude of χ_w are shown in Figs. 4 and 5 respectively. In these plots, the damping factor η was set to 10^{-3}. Now an increasing cross-correlation results in a degraded estimation performance. On the other hand, increasing ρ_{eff} leads to an improvement in the variance. Therefore, we see that for small τ, the SNR is essentially flat at the start, whereas $|\chi_w|$ is increasing (due to the action of the decaying window). Therefore, the optimal performance occurs for smaller r, and $r_{\min}$. As τ increases, however, the cross-correlation is seen to peak and then decrease (as the window flattens out and more independent noise samples are added.) Therefore, the performance for large τ is largely determined by ρ_{eff}, which always peaks at $r = 1$. As a result we see that for small τ a value of r smaller than 1 gives the best variance. This value increases towards 1 as τ increases.

Now using regression on Fig. 2, we obtain

$$f(\tau) \approx \begin{cases} 0.02\tau^2 + 0.02\tau + 0.39 & 0 < \tau \leq 3 \\ 1 - 1.08e^{-0.41\tau} - 0.07e^{-0.08\tau} & \tau > 3. \end{cases} \tag{30}$$

The approximation curve is included in Fig. 2 as the dash line and the resulting approximate ratio of minimum variance of η to the CRLB is also shown in Fig. 3. We can clearly see

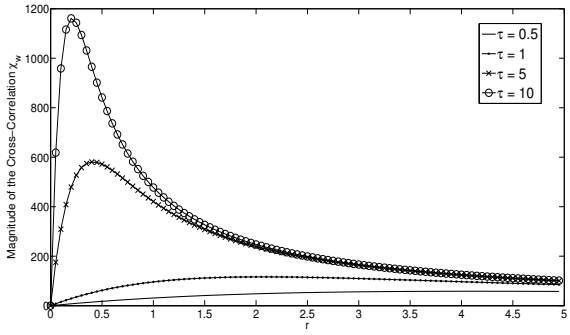

Fig. 5. Plot of the magnitude of the cross-correlation $|\chi_w|$ as a function of r under different values of τ (η = 0.001).

that after approximation of $r_{\min}$, the theoretical variance fits closely the curves obtained through simulations.

IV. Iterative Implementation

In the previous section we showed that the theoretical variances of the windowed estimator are extremely close to the CRLB if the decay factor of the window is properly chosen based on τ (that is on N and η). However, η has to be determined during the estimation process. We achieve this through an iterative implementation of the windowed estimator.

The iterative process is summarised in Table I. The original A&M estimator is applied in the first iteration. Then for all consecutive iterations, the previous residual estimates are removed from the maximum bin and the windowed estimator is applied after updating γ using the previous estimate of η. Based on the statistical analysis of the estimator, and using the convergence criteria discussed in [1] and [11], we stop the estimation process after two iterations.

V. Simulation Results

In this section, we present simulation results of the windowed estimator. In all cases, we implement both the exact

TABLE I
THE ITERATIVE WINDOWED ESTIMATOR

1. Calculate $X[n] = FFT(x)$;
2. Find $\hat{m} = \arg\max_n |X[n]|^2$;
3. Initialise $\hat{\delta}_0 = 0$, $\hat{\eta}_0 = 0$, and $\gamma = 0$;
4. For i from 1 to Q, do:
(1) Calculate $X_{\pm 0.5} = \sum_{k=0}^{N-1} x[k] e^{-\gamma k - j2\pi\left(\frac{\hat{m}+\hat{\delta}_{i-1} \pm 0.5}{N} k\right)}$
(2) Find $\hat{z}_\gamma$ using (4) and $\hat{\delta}_i = \hat{\delta}_{i-1} + \frac{N}{2\pi}\angle\hat{z}_\gamma$, $\hat{\eta}_i = -\ln\left(\hat{z}_\gamma\right) - \gamma$
(3) Calculate $\tau = N\hat{\eta}_i$ and find r using (30)
(4) Update $\gamma = r\hat{\eta}_i$;
5. Finally $\hat{f} = \frac{\hat{m} + \hat{\delta}_Q}{N}$, $\hat{\eta} = \hat{\eta}_Q$.

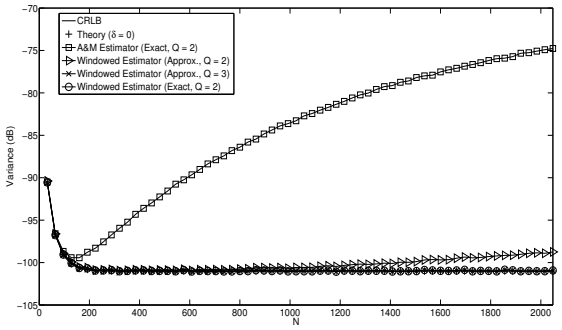

Fig. 6. Plot of the variance of the estimates of the frequency as a function of the number of samples N ($\eta = 0.02$, $\rho_0 = 40$dB). 10,000 Monte Carlo runs were used.

version given in (6) and the linearised estimator given in [1],

$$\hat{\eta} \approx \frac{2\pi}{N}\mathcal{I}(h) - \gamma, \quad \text{and} \quad \hat{\delta} = \mathcal{R}(h). \tag{31}$$

For the sake of comparison, we also include the performance of the exact version of the original A&M estimator, the CRLB as well as the theoretical variances obtained for $\delta = 0$ and r set according to Eq. (30). In each Monte Carlo run, the frequency is selected randomly.

Figs. 6 and 7 give the estimation variances of frequency and decay factor versus the number of samples N. It is evident that both the exact and linearised versions of the windowed

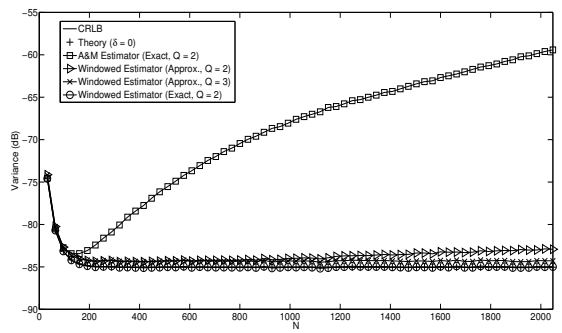

Fig. 7. Plot of the variance of the estimates of the decay factor as a function of the number of samples N ($\eta = 0.02$, $\rho_0 = 40$dB). 10,000 Monte Carlo runs were used.

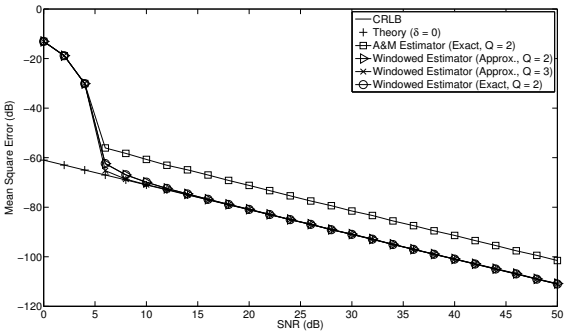

Fig. 8. Plot of the mean square error of the estimates of the frequency as a function of nominal SNR ρ_0 ($\eta = 0.02$, $N = 512$). 10,000 Monte Carlo runs were used.

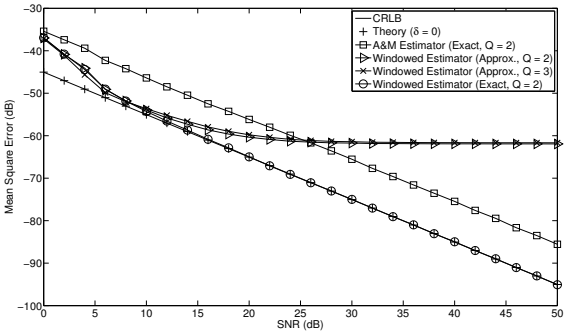

Fig. 9. Plot of the mean square error of the estimates of the decay factor as a function of nominal SNR ρ_0 ($\eta = 0.02$, $N = 512$). 10,000 Monte Carlo runs were used.

estimator outperform the original A&M algorithm. Whereas the original algorithm diverges wildly from the CRLB, the windowed estimators track it closely. Now comparing the exact and linearised versions, we see that the latter sacrifices performance for added computational simplicity. Thus its performance after 2 iterations exhibits a slight deviation from the theoretical curve for large N. This deviation can be reduced by running the linearised estimator for 3 iterations, but as we will see, this does not eliminate the bias in the estimates of the decay factor.

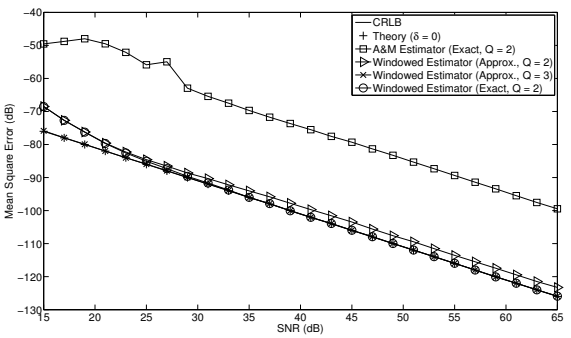

Fig. 10. Plot of the mean square error of the estimates of the frequency as a function of nominal SNR ρ_0 ($\eta = 0.02$, $N = 2048$). 10,000 Monte Carlo runs were used.

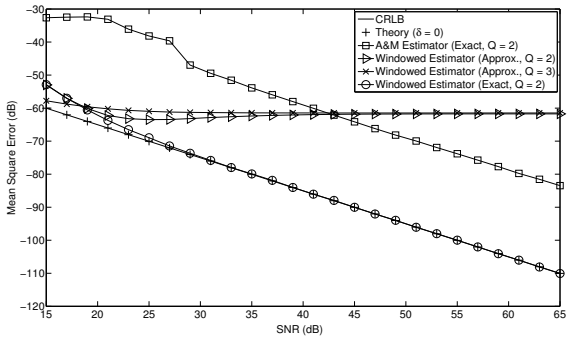

Fig. 11. Plot of the mean square error of the estimates of the decay factor as a function of nominal SNR ρ_0 ($\eta = 0.02$, $N = 2048$). 10,000 Monte Carlo runs were used.

The performance of the estimator as a function of SNR is shown in Figs. 8-11. The first two figures are obtained with $N = 512$, whereas the last two figures are for $N = 2048$. The same decay factor $\eta = 0.02$ is used throughout. In all four cases, it can be seen that the exact version of the estimator eliminates the problem of the original algorithm and exhibits a performance that sits on the CRLB. As a comparison, we note from Figs. 6 and 7 that the loss in performance of the original A&M algorithm with respect to the CRLB is about 8dB for $N = 512$, and about 25dB for $N = 2048$. Finally, although the linearised version shows significantly improved frequency estimation, the estimates of the damping factor exhibit a large bias that is clearly visible at high SNR.

VI. Conclusions

In this work we presented and analysed a novel algorithm for the estimation of the frequency and decay factor of a damped complex exponential in noise. In particular, we considered the A&M estimator, developed by Aboutanios and Mulgrew, and addressed the problem of performance degradation as the number of samples used in the estimation increases. To this end, we introduced a windowing strategy into the algorithm and showed that the best window is a decaying exponential. We presented theoretical analysis of the performance of the new algorithm and showed that it can track the CRLB if the window decay factor is appropriately chosen. Further, we determined the optimal value of the window decay factor and showed that it should be chosen based on the product of the number of samples and the signal damping decay. This strategy then requires knowledge of the signal decay factor, which is not available *a priori* and is to be estimated. Therefore, we addressed this issue by adopting an iterative implementation of the algorithm to find the appropriate window decay factor. Finally, we presented extensive simulation results that confirmed the theoretical results and demonstrated the significant improvement in the estimation performance.

References

[1] E. Aboutanios, "Estimation of the Frequency and Decay Factor of a Decaying Exponential in Noise," *Signal Processing, IEEE Transactions on*, vol. 58, no. 2, pp. 501–509, Feb. 2010.

[2] K. Duda, L.B. Magalas, M. Majewski, and T.P. Zielinski, "DFT-based estimation of damped oscillation parameters in low-frequency mechanical spectroscopy," *Instrumentation and Measurement, IEEE Transactions on*, vol. 60, no. 11, pp. 3608 –3618, nov. 2011.

[3] T.P. Zielinski and K. Duda, "Frequency and damping estimation methods - an overview," *Metrology and Measurement Systems*, vol. 18, no. 4, pp. 505–528, 2011.

[4] Y.X. Yao and S.M. Pandit, "Cramer-Rao lower bounds for a damped sinusoidal process," *Signal Processing, IEEE Transactions on*, vol. 43, no. 4, pp. 878–885, Apr 1995.

[5] F. Qian, S. Leung, Y. Zhu, W. Wong, D. Pao, and W. Lau, "Damped sinusoidal signals parameter estimation in frequency domain," *Signal Processing*, vol. 92, no. 2, pp. 381 – 391, 2012.

[6] F. K.W. Chan, H.C. So, and W. Sun, "Subspace approach for two-dimensional parameter estimation of multiple damped sinusoids," *Signal Processing*, vol. 92, no. 9, pp. 2172 – 2179, 2012.

[7] E. Aboutanios, Y. Kopsinis, and D. Rubtsov, "Instantaneous frequency based spectral analysis of nuclear magnetic resonance spectroscopy data," *Computers and Electrical Engineering*, vol. 38, no. 1, pp. 52–67, 2012.

[8] Y. Y. Lin, P. Hodgkinson, M. Ernst, and A. Pines, "A Novel Detection-Estimation Scheme for Noisy NMR Signals: Applications to Delayed Acquisition Data," *Journal of Magnetic Resonance*, vol. 128, no. 1, pp. 30 – 41, 1997.

[9] D. Rife and R. Boorstyn, "Single tone parameter estimation from discrete-time observations," *Information Theory, IEEE Transactions on*, vol. 20, no. 5, pp. 591–598, Sep 1974.

[10] B. G. Quinn and E. J. Hannan, *The estimation and tracking of frequency*, Cambridge University Press, New York, 2001.

[11] E. Aboutanios and B. Mulgrew, "Iterative frequency estimation by interpolation on Fourier coefficients," *IEEE Transactions on Signal Processing*, vol. 53, no. 4, pp. 1237–1242, Apr. 2005.

[12] C. Wu, "Asymptotic Theory of Nonlinear Least Squares Estimation," *Annals of Statistics*, vol. 9, no. 3, pp. 501–513, 1981.

[13] I. Yoshida, T. Sugai, S. Tani, M. Motegi, K. Minamida, and H. Hayakawa, "Automation of internal friction measurement apparatus of inverted torsion pendulum type," *Journal of Physics E: Scientific Instruments*, vol. 14, no. 10, pp. 1201, 1981.

[14] M. Bertocco, C. Offelli, and D. Petri, "Analysis of Damped Sinusoidal Signals via a Frequency-Domain Interpolation Algorithm," *Instrumentation and Measurement, IEEE Transactions on*, vol. 43, no. 2, pp. 245–250, Apr. 1994.

[15] E. Aboutanios, "Windowed iterative estimation of the parameters of damped complex exponentials in noise," in *Accepted for presentation at the European Signal Processing Conference, EUSIPCO 2013*, 2013.

[16] P. Stoica and T. Sundin, "Nonparametric NMR Spectroscopy," *Journal of Magnetic Resonance*, vol. 152, pp. 57–69, 2001.